TRENDS IN SCIENCES 2026; 23(7): 12535
https://doi.org/10.48048/tis.2026.12535 RESEARCH ARTICLE

Synthesis of Betacyanin-Grafted Inulin as a Colon Cancer Therapeutic: *In Silico* Evaluation via Molecular Docking and Molecular Dynamics

Minda Azhar[1,2,*], Selvi Apriliana Putri[3], Iman Permana Maksum[3], Rendi Ananda[4], Muhammad Habibul Iksan[3], Anni Faridah[5], Hastria Effendi[6] and Fatma Sri Wahyuni[7]

[1]*Department of Chemistry, Faculty of Mathematics and Natural Sciences, Universitas Negeri Padang, Padang 25131, Indonesia*
[2]*Molecular Biotechnology and Bioinformatics Research Centre, Indonesia*
[3]*Department of Chemistry, Faculty of Mathematics and Natural Sciences, Padjadjaran University, Bandung 40173, Indonesia*
[4]*PT. QL Agrofood Indonesia, West Java 17153, Indonesia*
[5]*Department of Culinary Arts, Faculty of Tourism and Hospitality, Universitas Negeri Padang, Padang 25131, Indonesia*
[6]*Department of Health and Recreation, Faculty of Sports Science, Universitas Negeri Padang, Padang 25131, Indonesia*
[7]*Faculty of Pharmacy, Andalas University, Kampus Limau Manis, Padang 25163, Indonesia*

([*]Corresponding author's e-mail: minda@fmipa.unp.ac.id)

Received: 5 November 2025, Revised: 7 December 2025, Accepted: 17 December 2025, Published: 20 February 2026

Abstract

Inulin is a fructan polymer composed of β-2,1-linked fructose units, known for its resistance to digestion in the upper gastrointestinal tract and selective fermentation by probiotics in the colon. This property makes inulin a promising candidate for colon-targeted drug delivery. In this study, betacyanin-grafted inulin was synthesized and evaluated for its potential as a colon cancer therapeutic, targeting Cyclooxygenase-2 (COX-2), a key enzyme involved in inflammation and tumor progression. This study aims to synthesize betacyanin-grafted inulin, characterize its structural and optical properties using Fourier Transform Infrared (FTIR) and Ultraviolet-Visible (UV-Vis) spectroscopy, assess its antioxidant activity, and evaluate its interaction with the COX-2 receptor through in silico molecular docking and molecular dynamics analysis. The grafting process was conducted under inert conditions using betacyanin masses of 0.2, 0.4 and 0.6 g. The optimal formulation was identified at 0.4 g, yielding a bound betacyanin content of 582 mg BAE/g. Structural characterization using FTIR revealed absorption bands at 1,540 - 1,418 cm^{-1} (C=C aromatic stretching) and 1,670 cm^{-1} (N-H bending), confirming the presence of betalamic acid. UV-Vis spectroscopy showed a maximum absorption at 530 nm, consistent with betacyanin's chromophore. Antioxidant assays demonstrated that the 0.4 g variation retained significant activity (35.08 mg/L), indicating that betacyanin remained bioactive post-grafting. In silico molecular docking and dynamics simulations revealed that betanin, the major betacyanin component, exhibited strong binding affinity (−8.6 kcal/mol) and favorable binding free energy (−20.3618 kcal/mol) at the COX-2 active site, suggesting stable interaction and potential inhibitory effects. ADMET analysis further supported the therapeutic viability of betacyanin, showing optimal absorption, wide distribution, and low predicted toxicity. These findings highlight the potential of betacyanin-grafted inulin as a natural, colon-targeted therapeutic strategy for COX-2-mediated colon cancer, combining targeted delivery with antioxidant and anti-inflammatory properties.

Keywords: Betacyanin, Inulin, Colon cancer, Drug delivery, Molecular docking, Molecular dynamics, ADMET, Cyclooxygenase-2 (COX-2)

Introduction

Inulin is the second most abundant polysaccharide in nature, after cellulose, and is found in various plants, including dahlia. The plant is a potential inulin source in Indonesia, particularly in highland regions such as Solok, Dieng, Malang, and Toraja. Inulin from Dahlia tuber (*Dahlia sp*) has been successfully extracted and characterized [1]. Inulin is a polymer composed of fructose monomers with a terminal glucose unit at the end of its molecular chain. The 3 hydroxyl groups attached to each fructose unit function as anchoring sites for further chemical modifications [2,3]. Inulin exhibits unique characteristics as it is not digested in the human stomach or small intestine but is instead metabolized by probiotics in the colon, leading to the production of short-chain fatty acids (SCFAs), which have various health benefits, including anti-cancer properties [4-6]. Due to these properties, inulin holds great potential as a drug delivery system, particularly for colon-related diseases. Colon-targeted therapy presents significant challenges as drug absorption often occurs in the stomach and small intestine, preventing the drug from effectively reaching the colon [7,8]. One promising strategy to overcome this limitation is to conjugate therapeutic agents with inulin, ensuring targeted drug release in the colon.

One of the major diseases affecting the colon is colon cancer, which is often associated with chronic inflammation, where the enzyme Cyclooxygenase-2 (COX-2) plays a central role in its pathogenesis. COX-2 is an enzyme involved in the biosynthesis of prostaglandins, molecules that regulate inflammation, cell proliferation, angiogenesis, and apoptosis resistance [9]. Elevated COX-2 expression has been detected in colon cancer tissues, particularly in both early and advanced stages, contributing to cancer cell growth, metastasis, and immune suppression within the tumor microenvironment [10]. Consequently, COX-2 inhibition has emerged as a promising therapeutic strategy for colon cancer treatment, either as a monotherapy or in combination with chemotherapy agents. However, conventional approaches using synthetic nonsteroidal anti-inflammatory drug (NSAID) inhibitors are frequently associated with cardiovascular and gastrointestinal side effects. Therefore, there is a need for a safer and more selective drug delivery strategy to target COX-2 while minimizing adverse effects effectively [11].

One of the organic compounds that has been successfully grafted onto inulin is catechin. Catechin-grafted inulin has been synthesized and characterized, demonstrating significant potential in anti-diabetic activity through *in vitro* studies [12]. Catechin, classified as a flavonoid and polyphenol, is known for its various health benefits, particularly in regulating blood glucose levels. Similarly, the synthesis of quercetin-grafted inulin has also been successfully synthesized in our previous study [13]. On the other hand, betacyanins, a pigment belonging to the betalain group, exhibit biological activities beneficial for the treatment of degenerative diseases, including cancer, cardiovascular diseases [14], heart disease, diabetes [15], and obesity [16]. Betanin, the primary component of betacyanin, has also been shown to play a role in colon cancer prevention [17]. However, betacyanins, composed of betanin and isobetanin, suffer from chemical instability, which limits their long-term therapeutic applications [18]. To overcome this limitation, inulin is a naturally occurring polysaccharide found in many plants, as a drug delivery system is highly relevant [19]. Inulin can enhance the stability of active compounds such as betacyanin, allowing for more efficient targeted delivery to the colon, the primary site for colon cancer treatment [20]. Beyond its role in grafting, encapsulating S-Adenosylmethionine (SAMe) in inulin nanoparticles has been identified as a promising strategy for colon-targeted drug delivery [21]. An innovative approach, such as the development of betacyanin-grafted inulin, has been proposed as a dual-function therapy, acting both as a prebiotic [22] and an efficient anti-cancer agent. Acetylating inulin increases its hydrophobicity, thus enabling the targeted delivery of 5-aminosalicylic acid to the intestine [23]. The synthesis of betacyanin-grafted inulin has not yet been reported; however, this approach holds great promise for advancing inulin-based drug delivery systems for cancer therapy, particularly in colon cancer treatment. To evaluate its potential, the study includes comprehensive testing comprising antioxidant activity assays, molecular docking, molecular dynamics simulations, and ADMET profiling.

Materials and methods

Materials

The materials used in this study include red dragon fruit peel (*Hylocereus sp.*) purchased from Padang, West Sumatra, along with ethanol, distilled water (aquades), inulin, and ascorbic acid. Additional reagents and consumables include Whatman filter paper No. 4, hydrogen peroxide, nitrogen gas, 80% ethanol solution, and an ethanol-water mixture (1:1). For analytical procedures, DPPH (2,2-diphenyl-1-picrylhydrazyl) reagent, Folin-Ciocalteu reagent, and sodium carbonate (Na_2CO_3) were utilized.

Sample preparation

Five kg of red dragon fruit peel was dried in an oven at 42 °C for 24 h. The dried sample was then ground and sieved using a 30-mesh sieve [24].

Betacyanins extraction

Betacyanin extraction was carried out following the procedure described by Fathordoobady *et al.* [24]. Two hundred and fifty g of dried and sieved red dragon fruit peel (Hylocereus sp.) was dissolved in 2.5 L of water and ethanol (1:1 ratio) and stirred at 900 rpm for 16 h. The mixture was then filtered using Whatman No. 4 filter paper, centrifuged at 10,000 rpm for 15 min at 4 °C, and concentrated under a vacuum using a rotary evaporator at 35 °C until thickened, followed by a drying process.

Characterization of betacyanin using FTIR and UV-Vis spectrophotometer

The betacyanin extract and betacyanin standard (Sigma Aldrich) were analyzed using Fourier Transform Infrared Spectroscopy (FTIR) in the wavenumber range of 600 - 4,000 cm^{-1} [25]. The betacyanins extract and betacyanin standard at a concentration of 1,000 mg/L were measured for absorbance in the range of wavelengths from 400 - 600 nm using UV-Vis (Ultraviolet-Visible) spectroscopy.

Synthesis of betacyanin-grafted inulin

Betacyanin-grafted inulin was synthesized following the procedure described by Liu *et al.* [12]. The grafting process was carried out using ascorbic acid and hydrogen peroxide (H_2O_2) under an inert atmosphere. Half g of inulin was dissolved in 25 mL of distilled water in a 50 mL 3-neck flask. Subsequently, 2 mL of 0.2 M hydrogen peroxide (H_2O_2) solution was added, and nitrogen gas was passed through the reactor for 30 min while stirring. Next, 0.2 g of betacyanin was introduced into the reactor, and the reaction was carried out under an oxygen-free nitrogen atmosphere for 12 h. The reaction mixture was then dialyzed using a 2,000 Da molecular cutoff membrane for 72 h to remove any unreacted betacyanin, followed by a drying process. The procedure was repeated for betacyanins variations of 0.4 g and 0.6 g to optimize the grafting process.

Characterization of betacyanin-grafted inulin using FTIR and UV-Vis spectrophotometer

Dried betacyanin-grafted inulin samples from different variations, along with betacyanin and inulin, were analyzed using FTIR within the frequency range of 600 - 4,000 cm^{-1} [26]. Additionally, each sample, including betacyanin-grafted inulin, betacyanin, and inulin, was prepared at a concentration of 1,000 mg/L, and their absorbance was measured within the wavelength range of 400 - 600 nm using UV-Vis spectroscopy.

Determination of betacyanin content in betacyanin-grafted inulin synthesis

The betacyanins binding content in betacyanin-grafted inulin was measured using the Folin-Ciocalteu method with slight modifications [26]. A 100 mg/L standard solution was prepared by dissolving 10 mg of betacyanin in ethanol in a 100 mL volumetric flask, and the volume was adjusted to the mark. Standard solutions of varying concentrations (5, 10, 20, 30, 40, and 50 mg/L) were then prepared. Each 1 mL of standard solution was mixed with 1 mL of Folin-Ciocalteu reagent (10-fold dilution) and allowed to react for 5 min. Then, 2 mL of 7.5% Na_2CO_3 solution was added. The mixture was incubated for 2 h, and the absorbance was measured at 760 nm. For sample analysis, 10 mg of betacyanin-grafted inulin from different variations was dissolved in distilled water in a 100 mL volumetric flask up to the mark. One mL of each sample solution was mixed with 1 mL of Folin-Ciocalteu reagent (10-fold dilution) and allowed to react for 5 min, followed by the addition of 2 mL of 7.5% Na_2CO_3 solution. The mixture was incubated for 2 h, and the absorbance was measured at 760 nm.

Antioxidant activity assay of betacyanin-grafted inulin using DPPH

The antioxidant activity of betacyanin-grafted inulin was evaluated using ascorbic acid and betacyanin standard as positive controls. Ten mg of ascorbic acid was dissolved in 80% ethanol within a 100 mL volumetric flask. Standard solutions at concentrations of 10, 20, 30, 40, and 50 mg/L were prepared to establish a calibration curve. Two mL of each concentration was transferred into test tubes and 3 mL of 0.1 mM DPPH solution. The mixture was then incubated for 1 h in the dark to prevent light exposure. The absorbance was measured at 517 nm using a UV-Vis spectrophotometer.

Preparation of betacyanin-grafted inulin test solution

Ten mg of betacyanin-grafted inulin was dissolved in 80% ethanol within a 100 mL volumetric flask. Different concentrations of betacyanin-grafted inulin solutions (10, 20, 30, 40, and 50 mg/L) were prepared. Two mL of each concentration was transferred into test tubes and 3 mL of 0.1 mM DPPH solution. The mixture was then incubated for 1 h in the dark. The absorbance was measured at 517 nm using a UV-Vis spectrophotometer. The blank solution was 80% ethanol, while DPPH without the test sample (3 mL of DPPH + 2 mL of 80% ethanol) served as the control. The antioxidant activity (%) was calculated using the following formula [24].

$$\%Antioxidant\ Activity = \left(\frac{Absorbance\ of\ Control - Absorbance\ of\ Sample}{Absorbance\ of\ Control}\right) \times 100\%$$

Molecular docking

The crystal structure of Cyclooxygenase-2 (COX-2) from Mus musculus was retrieved from the Protein Data Bank (PDB ID: 6COX) and used as the initial model for molecular docking simulations. The 3-dimensional (3D) structures of the ligand compounds, betacyanin (betanin and isobetanin), were prepared using ChemBioDraw Ultra 12.0 in a water-free state to ensure optimal structural conditions before docking. Molecular docking simulations were performed using AutoDock Vina, beginning with the preparation of the enzyme and ligand. In this stage, all unnecessary components, such as water molecules and heteroatoms (e.g., additional ligands present in the crystallographic enzyme structure), were removed from the enzyme.pdb file. Before docking, polar hydrogen atoms were added to the structure to enhance the accuracy of ligand-protein interactions. The protein-ligand interaction model with the lowest docking energy was selected as the best model, as it represents the most thermodynamically stable and favorable binding mode. The resulting protein-ligand complex was further analyzed to evaluate residual changes within the enzyme's active site. Molecular interactions between the ligand and COX-2 active site residues were visualized using PyMOL and Discovery Studio, allowing for the identification of bond types between the ligand and receptor.

Molecular dynamics simulation

MD simulations were performed in Amber20 for 2 protein-ligand complexes. Each system was prepared using the LEaP module: The protein was parameterized with the ff14SB force field and the ligands with gaff2. The complexes were solvated in a periodic box of TIP3P water molecules and neutralized with Na^+ ions. Energy minimization was conducted in 3 sequential stages: First on the solvent (2,000 cycles), then on the protein (2,000 cycles), and finally on the entire system (4,000 cycles). The minimized system was gradually heated from 0 to 37 °C under weak harmonic restraints, followed by a 200 ps equilibration phase in the NPT ensemble. Production MD was subsequently run for 200 ns under NPT conditions. The binding free energy was calculated using the MMGBSA.py module in Amber20 on the combined production trajectory, from which water molecules and ions had been stripped.

ADMET and lipinski rules analysis

The pharmacokinetic properties and toxicity profiles of betanin and isobetanin were assessed using SwissADME (http://www.swissadme.ch/) and pkCSM (https://biosig.lab.uq.edu.au/pkcsm/) web server to evaluate their oral bioavailability and potential side effects. Pharmacokinetics constitutes a quantitative framework for characterizing the processes of drug absorption, systemic distribution, and elimination, which collectively determine the temporal profile of pharmacodynamic responses following administration.

Results and discussion

Extraction and identification of betacyanins from red dragon fruit peel

Betacyanins are natural red pigments predominantly found in the peel of red dragon fruit (*Hylocereus sp.*). These compounds belong to the betalain group and exhibit high antioxidant potential. Betacyanins are polar molecules due to the presence of hydroxyl (-OH) groups, which facilitates their extraction using polar solvents, such as an ethanol-water mixture (1:1) [27]. The selection of this solvent aims to maximize the yield of bioactive compounds while ensuring the stability of betacyanins throughout the extraction process. The betacyanins content extracted from red dragon fruit peel was 28.44 mg/100 mL [24]. In this study, the extraction of 250 g of dragon fruit peel yielded 5 g of dried betacyanin extract, indicating a relatively high extraction efficiency compared to alternative solvent-based methods.

The characterization of betacyanins compounds in the extract was performed using 2 primary analytical methods such as; FTIR and UV-Vis Spectrophotometry. In this analysis, standard betacyanin was also used. FTIR analysis was conducted to identify the functional groups present in betacyanins, ensuring the presence of their characteristic structural components. The FTIR spectrum of betacyanins is presented in **Figure 1**, displaying the key functional groups that define the molecular structure of betacyanins.

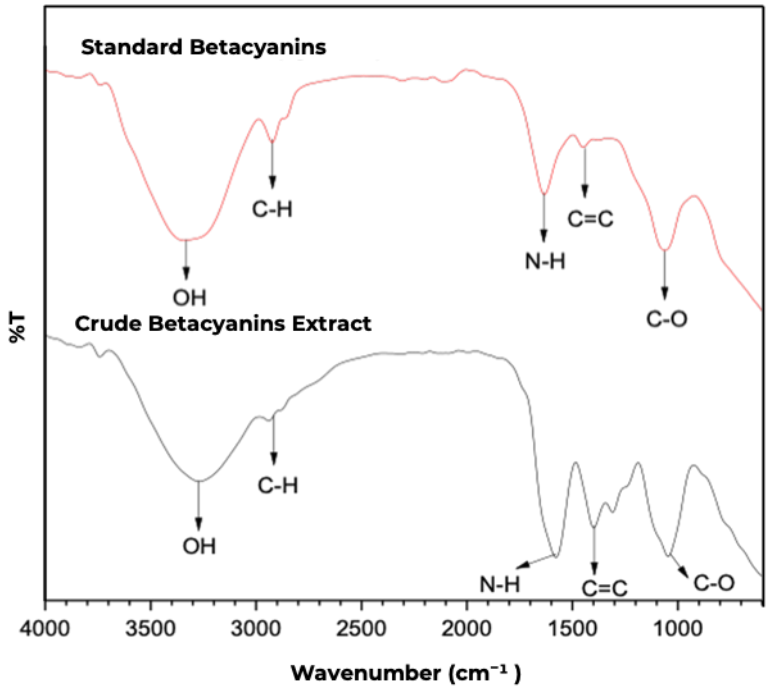

Figure 1 FTIR Spectra of standard betacyanin (betanin) and betacyanins extract from red dragon fruit peel.

A broad absorption band observed in the wavenumber range of 3,681 - 3,000 cm^{-1} corresponds to the O-H stretching vibrations of carboxylic acids, which are characteristic of phenolic compounds in betacyanins. The presence of this band indicates the occurrence of hydrogen bonding interactions within the betacyanin structure, contributing to its stability under various environmental conditions. Furthermore, absorption bands observed in the range of 1,798 - 1,607 cm^{-1} indicate the presence of N-H functional groups attributable to betalamic acid, a core structural component of betacyanin. This finding confirms that betacyanins in the extract retain an intact betalain core, which is essential for its biological activity, particularly its antioxidant and anti-cancer properties [17].

An absorption band at 1,486 cm^{-1} corresponds to the C=C stretching vibrations of the aromatic ring, indicating the presence of a conjugated structure within betacyanins. The presence of this band confirms the

existence of double bonds in the aromatic structure, which contribute to its optical properties, including its ability to absorb light in the wavelength range of 530 - 538 nm. Another notable absorption band observed in the range of 1,470 - 1,344 cm^{-1} is associated with C-O stretching vibrations, suggesting the presence of carboxylate or hydroxyl groups. These functional groups play a crucial role in enhancing the solubility of betacyanins in polar media, facilitating its extraction using polar solvents such as the ethanol-water (1:1) mixture employed in this study. Thus, FTIR analysis confirms that betacyanins extracted from red dragon fruit peel exhibits a spectral profile consistent with that of pure betacyanins, as reported in the literature [25]. The agreement between the obtained spectral data and the standard betacyanins spectrum further validates the successful extraction of betacyanins from dragon fruit peel. The characterization process was further extended to UV-Vis spectrophotometric analysis to assess its optical properties (**Figure S1**).

The UV-Vis spectra of the betacyanin extract and standard betacyanin illustrate the characteristic absorption pattern of betacyanin in an ethanol solvent medium. The spectral results exhibit a strong absorption band at 530 nm for both the betacyanin extract and the Sigma Aldrich standard, confirming that the major compound present in the extract is indeed betacyanin, which possesses well-defined optical characteristics, as previously reported in the literature [16]. Betacyanins are a red pigment belonging to the betalain group, commonly found in plants such as dragon fruit. The conjugated double bonds in the betalamic acid moiety of betacyanin function as chromophores, facilitating light absorption at a maximum wavelength of 530 nm [28]. This chromophore system enables betacyanin to absorb visible light in the green-blue region (approximately 530 nm), while transmitting red wavelengths, which accounts for the red coloration of the extract. The similarity in the absorption peaks between the betacyanin extract and the Sigma Aldrich standard indicates that the core structure of betacyanins remained intact during the extraction process. Furthermore, these findings confirm that the ethanol-based extraction method effectively preserves the stability of betacyanins, ensuring its structural integrity throughout the process. Furthermore, a sharp absorption peak at 530 nm indicates the stability of the betacyanins spectrum under the analytical conditions applied, with no observable spectral shifts. Bathochromic (red shift) or hypsochromic (blue shift) shifts often occur due to pH variations or interactions with other compounds. However, in this study, the absence of any wavelength shift between the betacyanins extract and the betacyanins standard suggests that the chemical structure of betacyanins in the extract remained intact, with no degradation occurring during the extraction and analysis process. Based on UV-Vis spectrophotometric measurements, the betacyanins extract displayed spectral features characteristic of pure betacyanin, confirming its compositional integrity. This validation suggests that the extract has potential applications in various fields, including natural colorants, dietary supplements, and further research on its antioxidant and anti-cancer activities.

Synthesis and betacyanins content in betacyanin-grafted inulin

In this study, betacyanins were successfully grafted onto inulin using an ascorbic acid and hydrogen peroxide (H_2O_2) system under a nitrogen gas flow. This reaction is based on the mechanism reported by Liu *et al.* [12], where ascorbic acid acts as a reducing agent, reacting with H_2O_2 to generate hydroxyl radicals (HO•) [26]. These radicals subsequently initiate the covalent binding of betacyanins to inulin, enhancing the stability of the resulting compound. Bound betacyanins content in the synthesized product was quantified via the Folin-Ciocalteu assay, employing slight procedural modifications. This method is based on a redox reaction between the Folin-Ciocalteu reagent - which initially appears yellow - and the phenolic groups present in betacyanin, resulting in the formation of a blue complex under alkaline conditions, which can be spectrophotometrically measured. The formation of this complex confirms the successful binding of betacyanins to the inulin.

To determine the bound betacyanins content in the synthesized betacyanin-grafted inulin, a standard calibration curve was established using various betacyanins concentrations to obtain a linear regression equation. The standard regression equation derived from this curve was $y = 0.0126x + 0.1986$ with a correlation coefficient (r) of 0.9872, indicating that 98.72% of the absorbance variation is influenced by betacyanins

concentration. This standard curve was then utilized to calculate the bound betacyanins content in betacyanin-grafted inulin by measuring the absorbance of each synthesized variation and applying the obtained regression equation (**Figure S2**).

The results of this study indicate that the highest betacyanins binding efficiency was achieved in the second synthesis variation (+ 0.4 g betacyanins), with a binding content of 582 mg BAE/g, as determined by the Folin-Ciocalteu method. This value is significantly higher than the previously reported catechin binding in catechin-grafted inulin, which was 124.8 mg CAE/g [26]. Bound betacyanins content in the first synthesis variation measured 289 mg BAE/g. This relatively lower value may be attributed to the presence of oxygen in the reaction system, which could have hindered the binding process with inulin. Additionally, betacyanins radicals may have undergone self-interaction, reducing the availability of reactive radicals for interaction with inulin radicals. For the third synthesis variation, the bound betacyanins content was 400 mg BAE/g, slightly lower than that of the second variation. This reduction may be due to an increase in solution viscosity during the reaction, which could have restricted the mobility of betacyanins radicals, thereby limiting their interaction with inulin radicals.

The quantification of bound betacyanins in the synthesized betacyanin-grafted inulin using the Folin-Ciocalteu method confirmed the successful binding of betacyanins to inulin through a radical reaction mechanism initiated by ascorbic acid and hydrogen peroxide under inert conditions (nitrogen gas flow). These findings demonstrate that the synthesis method employed was effective in producing betacyanin-grafted inulin with a high betacyanins content, highlighting its potential for applications in the food and pharmaceutical industries as a bioactive compound with strong antioxidant activity. Concentration Bound Betacyanins in Betacyanin-Grafted Inulin can be seen in **Table 1**.

Table 1 Bound betacyanins concentration in betacyanin-grafted inulin at different betacyanins concentrations.

No	Synthesis Variation	Concentration (ppm)	Absorbance	mg BAE/ g
1.	Variation 1 (+ 0.2 g Betacyanins)	100	0.235	289
2.	Variation 2 (+ 0.4 g Betacyanins)	100	0.272	582
3.	Variation 3 (+ 0.6 g Betacyanins)	100	0.249	400

Characterization of betacyanin-grafted inulin using FTIR and UV-Vis spectrophotometry

Fourier Transform Infrared (FTIR) spectroscopy and UV-Vis spectrophotometry were utilized to analyze the structural and optical properties of betacyanin-grafted inulin. FTIR spectra were recorded in the wavenumber range of 4,000 - 600 cm^{-1} to analyze vibrational changes in betacyanins, inulin, and betacyanin-grafted inulin. The FTIR spectrum of betacyanins exhibited characteristic phenolic compound features, with a broad absorption band at 3,437 cm^{-1}, corresponding to O-H stretching vibrations. Additionally, a sharp absorption band at 1,400 cm^{-1} was associated with C=C stretching vibrations from the aromatic ring of betacyanins. A strong absorption band at 1,600 cm^{-1} confirmed the existence of N-H groups from betalamic acid, while bands in the 1,200 - 1,300 cm^{-1} region were attributed to C-O stretching vibrations from carboxyl carbonyl bonds (Figure **2**). The consistency of these absorption bands in the sample indicates that the fundamental properties of betacyanin were preserved despite its interaction with inulin.

A strong absorption peak at 3,367 cm^{-1} in the FTIR spectrum of inulin corresponds to O-H stretching, indicative of polysaccharide structures. Additionally, an absorption band at 2931 cm^{-1} was associated with C-H stretching vibrations, while bands between 1,132 and 1,032 cm^{-1} corresponded to C-O stretching vibrations, indicating the presence of carbonyl functional groups within the inulin structure. Upon betacyanin-grafted inulin, distinct spectral changes were observed. The appearance of new absorption bands at 1,540 cm^{-1} and 1,418 cm^{-1} was associated with C=C stretching vibrations from the aromatic ring of betacyanins. Furthermore, a new absorption band at 1,670 cm^{-1} was observed, corresponding to the N-H bond of betalamic

acid in betacyanins [28]. These spectral shifts confirm the successful interaction between betacyanins and inulin, indicating that the system is not merely a physical mixture but a molecularly bonded complex, supported by hydrogen bonding interactions.

To further confirm the binding of betacyanin to inulin, UV-Vis spectrophotometry was performed to analyze the maximum absorption wavelength, providing evidence of structural integrity post-grafting [29]. The analysis was conducted within the wavelength range of 400 - 600 nm. The UV-Vis spectrum of betacyanins in ethanol solution displayed a strong absorption peak at 530 nm, attributed to the conjugated double bonds within the betalamic acid structure, which serves as the primary chromophore in betacyanins (**Figure S3**). In contrast, pure inulin solution exhibited no absorption peaks within this range, as inulin lacks chromophoric functional groups capable of absorbing UV-Vis radiation. Analysis of the UV-Vis spectrum for betacyanin-grafted inulin revealed a characteristic strong absorption within the 400 - 600 nm region. The maximum absorbance peak (λmax) was identified at 530 nm, confirming that the betacyanin molecules maintained their integrity and key optical properties despite being covalently bound to the inulin backbone [28]. The stability of this absorption peak further confirms that the betacyanin-grafted inulin was successfully formed without structural degradation, thereby preserving its functional bioactivity. Based on these characterization results, it can be concluded that betacyanins successfully interacted with inulin, as evidenced by FTIR spectral changes and the persistence of the absorption peak in the UV-Vis spectrum. The success of this interaction highlights inulin's potential as a natural pigment delivery matrix, enhancing the stability and efficacy of betacyanins for pharmaceutical applications, particularly in colon cancer treatment. Further investigation is necessary to investigate the thermal stability and degradation kinetics of betacyanin-grafted inulin, particularly under varying pH and temperature conditions, to evaluate its long-term stability and performance under various environmental conditions.

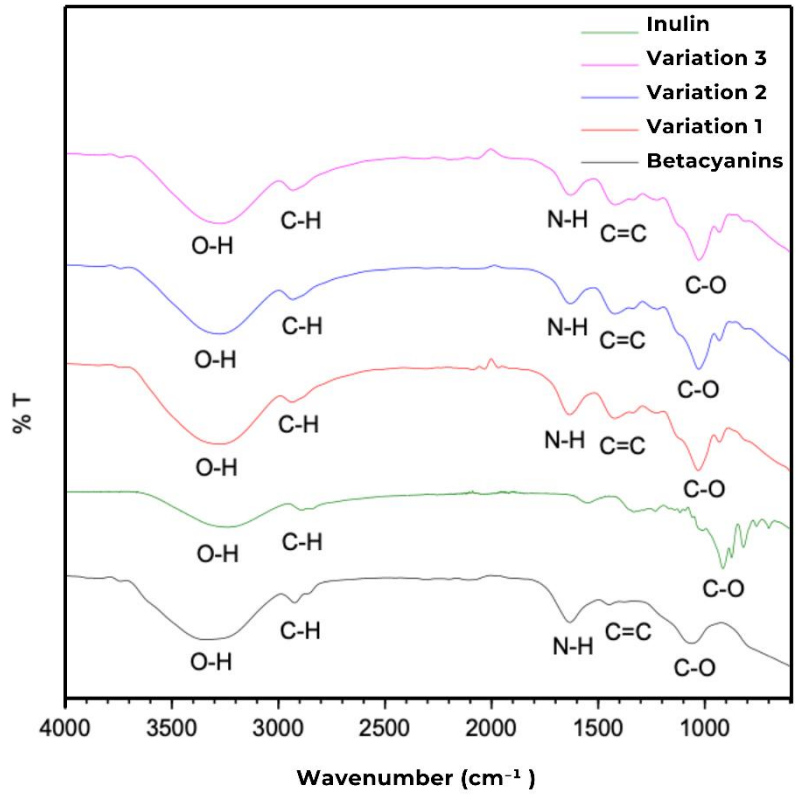

Figure 2 FTIR spectra of synthesized betacyanin, inulin, and betacyanin-grafted inulin.

Antioxidant activity of betacyanin-grafted inulin

The antioxidant activity of betacyanin-grafted inulin was assessed using the 2,2-diphenyl-1-picrylhydrazyl (DPPH) assay, a widely used method in antioxidant research due to its simplicity, rapid analysis, and minimal sample requirement. The stability of DPPH at room temperature, along with its characteristic purple hue, arises from the delocalization of an unpaired electron within its molecular structure. The fundamental principle of this method involves measuring the color change of the DPPH solution, which shifts from purple to yellow upon reaction with an antioxidant compound capable of donating an electron or hydrogen atom. The greater the observed color change, the higher the antioxidant activity of the tested compound.

The antioxidant activity of betacyanin-grafted inulin was evaluated using the DPPH assay at varying concentrations, with ascorbic acid and betacyanin serving as positive controls. The outcomes of the DPPH radical scavenging assay at different concentrations of betacyanin-grafted inulin, compared to the control samples, are depicted in a concentration-dependent inhibition curve (**Figure S4**). The findings indicate a progressive increase in DPPH radical inhibition (%) with increasing concentrations of betacyanin-grafted inulin, suggesting that higher concentrations exhibit greater free radical scavenging ability. This trend confirms the dose-dependent antioxidant potential of betacyanin-grafted inulin. The IC_{50} values for the different variations of betacyanin-grafted inulin and the positive controls are summarized in **Table 2**, providing a comparative assessment of their antioxidant effectiveness.

The analysis results indicate that the second betacyanin variation (0.4 g) in the synthesis of betacyanin-grafted inulin exhibited a lower IC_{50} value compared to the first and third variations. This finding suggests that the second variation possesses higher antioxidant activity. Ascorbic acid and betacyanin were used as positive controls to compare the antioxidant effectiveness of the synthesized betacyanin-grafted inulin. The obtained IC_{50} values further demonstrate a correlation between the bound betacyanin content in betacyanin-grafted inulin and its antioxidant activity. Specifically, a higher betacyanin content in the grafted inulin resulted in a lower IC_{50} value, indicating greater free radical scavenging potential. In general, antioxidant activity is classified as follows: very strong: $IC_{50} < 50$ ppm, strong: IC_{50} between 50 - 100 ppm, moderate: IC_{50} between 100 - 250 ppm and inactive: $IC_{50} > 250$ ppm [30]. The betacyanin-grafted inulin synthesized in this study exhibited strong antioxidant activity, with an IC_{50} value within the optimal range for effective free radical scavenging.

Table 2 Antioxidant activity measurements of betacyanin-grafted inulin.

Synthesis of Betacyanin grafted Inulin	IC_{50} (ppm)
Variation 1 (+ 0.2 g Betacyanin)	41.91
Variation 2 (+ 0.4 g Betacyanin)	35.08
Variation 3 (+ 0.6 g Betacyanin)	39.01
Ascorbic acid	4.43
Betacyanin	20.83

Inulin exhibits relatively weak antioxidant activity, with a DPPH radical inhibition rate of only 20.81% [31]. However, the results of this study demonstrate that binding inulin with betacyanins significantly enhances its antioxidant effectiveness, as evidenced by the reduction in IC_{50} values across all synthesis variations compared to pure inulin. This improvement can be attributed to intermolecular interactions that increase the stability of betacyanins and prolong their effectiveness as an antioxidant in physiological environments. Betacyanin-grafted inulin acts as a dual-function system, delivering bioactive compounds while providing potent antioxidant and prebiotic benefits. These findings suggest that betacyanin-grafted inulin has the potential to serve as an effective natural antioxidant source with promising applications in various industries, particularly in the

development of functional food ingredients and pharmaceutical products.

Molecular docking analysis

The molecular docking results indicate that celecoxib, betanin, and isobetanin exhibit distinct interactions within the active site of Cyclooxygenase-2 (COX-2). The binding affinity values obtained from the docking analysis reveal that celecoxib has the lowest binding energy at −11.5 kcal/mol, followed by betanin (−8.6 kcal/mol) and isobetanin (−7.8 kcal/mol). The negative binding affinity values suggest the strength of ligand binding to the target enzyme, with lower values indicating higher stability [32]. Based on these results, celecoxib exhibited the highest binding affinity to COX-2, exceeding that of betanin and isobetanin.

Visualization of molecular interactions shows that betanin interacts with key residues within the COX-2 active pocket, forming conventional hydrogen bonds with GLN A:192, PRO A:191, HIS A:351, ASN A:581, and PHE A:580 (**Figure 3**). Additionally, a salt bridge interaction with ASP A:347 was identified, which may enhance binding stability and strengthen the affinity of betanin toward the enzyme. This interaction pattern suggests that betanin has the potential to act as a competitive COX-2 inhibitor, capable of forming stable ligand-protein interactions.

Similar to betanin, isobetanin exhibited a comparable molecular interaction pattern within the COX-2 active site but with notable differences in the types of bonds formed. Isobetanin established conventional hydrogen bonds with SER A:579, ASP A:347, ASN A:581, PHE A:580, HIS A:351, GLN A:192, and TYR A:355. Additionally, the involvement of amide-π stacking interactions with aromatic residues in the COX-2 active pocket suggests that such interactions may contribute to complex stability. However, the docking analysis also identified the presence of unfavorable donor-donor hydrogen interactions, which could weaken the overall interaction strength and reduce the binding affinity of isobetanin compared to betanin. The binding affinity of isobetanin (−7.8 kcal/mol) was lower than that of both betanin (−8.6 kcal/mol) and celecoxib (−11.5 kcal/mol). This suggests that isobetanin exhibits weaker interaction stability, potentially due to a reduction in stable electrostatic interactions within the COX-2 binding site.

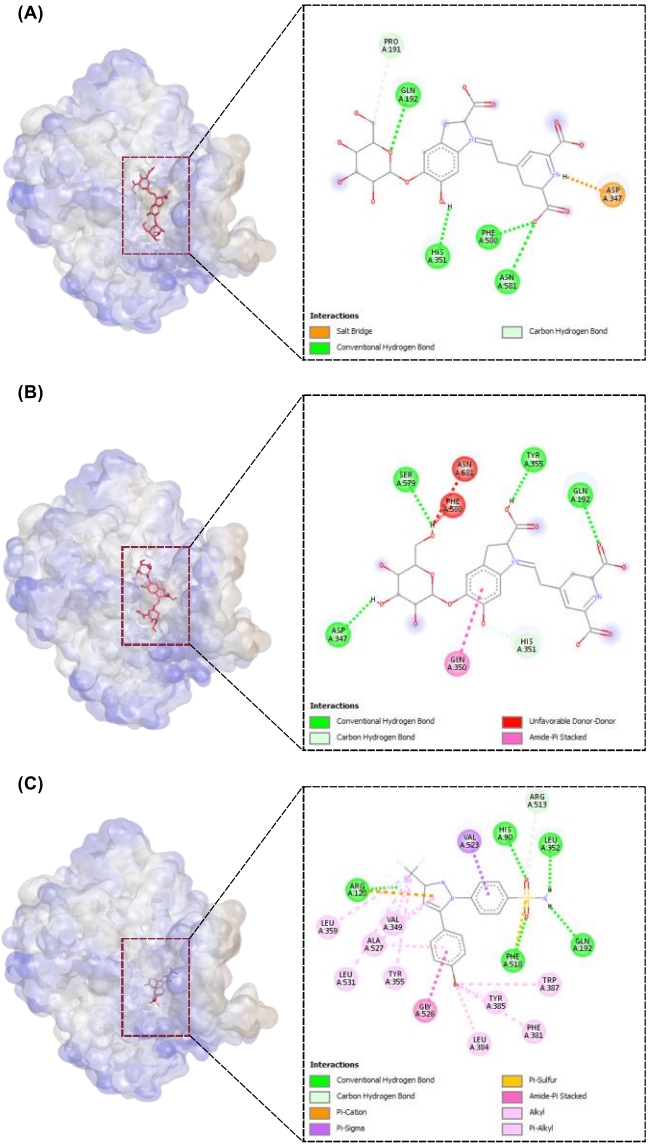

Figure 3 Molecular interaction visualization from targeted docking using discovery studio visualizer. molecular docking interactions of (A) betanin-COX-2, (B) isobetanin-COX-2, and (C) celecoxib-COX-2 demonstrate the binding orientations and key interactions within the COX-2 active site.

As a clinically established selective COX-2 inhibitor, celecoxib exhibited a more complex molecular interaction pattern compared to the natural compounds betanin and isobetanin. Celecoxib formed conventional hydrogen bonds with GLN A:192, HIS A:351, PHE A:581, and ARG A:513, along with multiple hydrophobic interactions, including π-π stacking, π-sulfur, and π-alkyl interactions, which contributed to ligand stability within the COX-2 active site. Additionally, π-cation and π-sigma interactions were identified with ARG A:120 and other hydrophobic residues, further enhancing the binding affinity of celecoxib to the enzyme. The interplay of hydrogen bonding and hydrophobic interactions renders celecoxib the most stable COX-2 inhibitor among the trio of compounds examined, thereby reinforcing its superior binding affinity in relation to betanin and isobetanin.

Based on the comparison of binding affinity values and molecular interaction types, it can be concluded that betanin exhibits greater potential than isobetanin in inhibiting COX-2 activity. However, its binding affinity and interaction stability remain inferior to celecoxib. The differences in binding affinity values suggest that, although betanin and isobetanin can interact with key residues within the COX-2 active pocket, their effectiveness is still lower than that of celecoxib. This

discrepancy may be attributed to the lack of significant hydrophobic interactions in betanin and isobetanin, whereas celecoxib benefits from a complex combination of hydrogen bonding, π-stacking, and electrostatic interactions, contributing to higher binding stability and affinity.

Although betanin demonstrates potential as a COX-2 inhibitor, further studies are required to optimize its inhibitory activity. In this study, betacyanin grafted inulin is expected to preserve its bioactivity, ensuring efficient delivery to the target protein. Inulin has been widely employed in pharmaceutical formulations due to its versatility as a drug carrier, stabilizing agent, and cryoprotectant, as well as its role as a functional alternative to fats and sugars in various applications [33,34]. Chemical modifications of betanin and isobetanin could be a promising approach to enhance their interaction stability and binding affinity toward COX-2. Additionally, further molecular dynamics simulations are needed to confirm the biological efficacy of these compounds in COX-2 inhibition. This study offers significant insights into the exploration of natural compounds as potential COX-2 inhibitors, underscoring their promise as natural anti-inflammatory agents with superior safety profiles compared to synthetic pharmaceuticals.

Molecular dynamics simulations

The molecular dynamics (MD) simulations conducted over 200 ns provided robust evidence of the differential stability and interaction modes of betanin and isobetanin with COX-2. Binding free energy calculations derived from the trajectory revealed that betanin displayed a substantially more favorable interaction energy (−20.3618 kcal/mol) compared to isobetanin (−11.9880 kcal/mol). This energetic advantage is mechanistically supported by the ability of betanin to establish and maintain an extensive hydrogen bonding network with critical residues within the catalytic pocket, including ASP316, GLY323, PHE549, HIE320, ASP484, GLN319, GLN534, and GLN552, for a total of nine hydrogen bonds. In contrast, isobetanin was only able to sustain a single hydrogen bond with ASP484 throughout the simulation, highlighting its relatively weaker anchoring within the binding site. The persistence and multiplicity of these interactions indicate that betanin is able to stabilize the microenvironment of the active site, thereby enhancing its inhibitory potential (**Table 3**).

Table 3 Binding free energy and hydrogen bond of betanin and isobetanin in MD simulation.

Compounds	Binding Free Energy (ΔG) (kcal/mol)	H Bond	Total
Betanin	−20.3618	ASP316, GLY323, PHE549, HIE320, ASP484, GLN319, ASP484, GLN534, GLN552	9
Isobetanin	−11. 9880	ASP484	1

Conformational stability analyses provided further support for these energetic findings. RMSD trajectories showed that the betanin-COX-2 complex rapidly converged to a stable conformation and maintained low fluctuations with a mean RMSD of 2.1 ± 0.3 Å, suggesting a highly consistent binding mode across the 200 ns simulation. In contrast, the isobetanin-COX-2 complex exhibited larger structural deviations, reflected in a mean RMSD of 2.8 ± 0.5 Å, consistent with weaker anchoring and less stable interactions within the active site. At the residue level, RMSF analysis demonstrated that betanin effectively constrained the mobility of catalytic and pocket-lining residues, reducing their flexibility with an average RMSF of 1.2 ± 0.2 Å. This stabilization is critical, as catalytic site rigidity often correlates with sustained inhibitory binding. By comparison, isobetanin binding induced higher residue-level fluctuations (average RMSF 1.7 ± 0.4 Å), particularly in loop regions surrounding the catalytic pocket, indicative of reduced stabilization and dynamic instability (**Figure 4**).

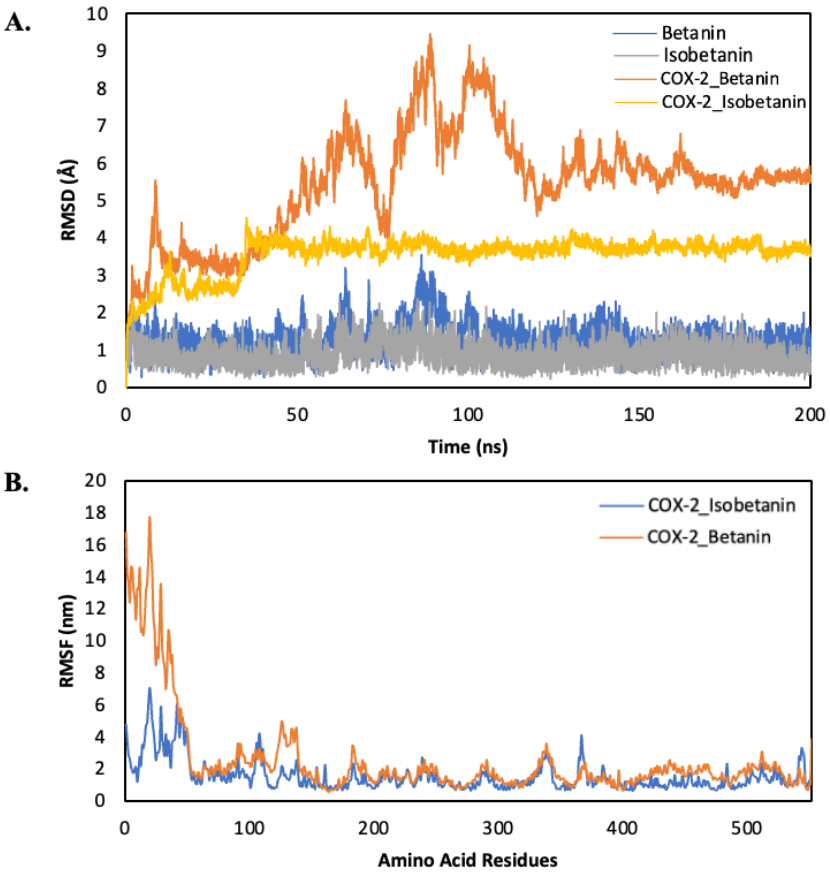

Figure 4 RMSD and RMSF profile. A) RMSD of Betanin and Isobetanin complex, B) RMSF COX-2_ Betanin and Isobetanin complex.

The integration of these simulation results provides a coherent mechanistic interpretation for the differential inhibitory potential of betanin and isobetanin against COX-2. The stronger binding free energy (ΔG) and persistent hydrogen-bonding network of betanin directly correlate with reduced conformational mobility of the enzyme, observed at both the global (RMSD) and local (RMSF) levels during molecular dynamics simulations. This stabilization is likely to impair the dynamic flexibility essential for COX-2's catalytic activity.

The mechanistic action of the COX-2 enzyme is highly dependent on the ability of its active site to undergo conformational changes to accommodate the substrate (arachidonic acid) and during the catalysis process [35]. This conformational sampling, particularly in flexible regions such as the gate loop, is critical for substrate turnover [36]. By restricting this conformational plasticity, betanin may act as an allosteric-like stabilizer that effectively suppresses enzyme function. This aligns with previous studies reporting that potent COX-2 inhibitors, such as celecoxib, often lock the enzyme in an inactive or less flexible conformational state. In contrast, isobetanin, with its weaker energetic interactions and limited hydrogen bonding, fails to exert the same degree of structural control. Consequently, the COX-2-isobetanin complex retains greater mobility, explaining its more modest inhibitory potential. This finding is consistent with the fund'mental principle that the stability of an enzyme-ligand complex is directly proportional to its inhibitory effectiveness [37].

From a therapeutic perspective, these findings are highly significant. COX-2 overexpression is strongly implicated in the pathogenesis of chronic inflammation, tumor progression, and colorectal carcinogenesis [38]. The ability of betanin to form a stable and energetically favorable complex with COX-2 suggests a potential mechanism for its anti-inflammatory and anticancer action, extending the understanding beyond its well-known antioxidant activity [39]. Its superior interaction profile compared to isobetanin positions betanin as a

more promising lead compound for further development in cosmeceutical (e.g., anti-aging or anti-inflammatory creams) or pharmaceutical contexts.

Furthermore, the strong concordance between molecular docking results, binding free energy (MMGBSA), hydrogen bond analysis, and long-timescale MD stability provides robust validation of betanin's inhibitory potential. This multi-level confirmation strengthens the candidacy of betanin for translational research aimed at developing natural products for selective and effective COX-2 inhibition.

ADMET and lipinski rules analysis

The pharmacokinetic properties and toxicity profiles of betanin and isobetanin were analyzed using SwissADME and pkCSM to evaluate their oral bioavailability and potential adverse effects (**Table 4**). A key differentiating factor among these compounds is their absorption and permeability properties, significantly influencing their bioavailability and therapeutic efficacy [40]. Celecoxib exhibits a high log P value (3.072), favoring lipophilicity, which enhances gastrointestinal (GI) absorption and systemic distribution, along with moderate solubility at physiological pH (log D 7.4 = 3.246), ensuring effective delivery to its target site. Conversely, betanin and isobetanin display lower log P values (−1.646 and −1.666, respectively), indicating a predominantly hydrophilic nature, which may limit their ability to cross lipid membranes and undergo passive diffusion, thereby reducing their absorption efficiency and systemic exposure. Nevertheless, these limitations can be effectively addressed through inulin-based encapsulation, which facilitates the controlled release of compounds in the colon, thereby ensuring precise delivery to the target site of action while reducing premature absorption in the upper gastrointestinal tract.

Despite celecoxib's GI absorption, betanin and isobetanin exhibit reduced oral bioavailability, necessitating a targeted delivery approach to enhance their therapeutic effects in the colon. Incorporating inulin, which undergoes microbial fermentation by gut microbiota, enables the precise release of active compounds at the site of colonic inflammation, thereby improving local bioavailability and pharmacological action. In terms of distribution, all 3 compounds demonstrate negative blood-brain barrier (BBB) permeability, suggesting a lower likelihood of central nervous system (CNS) side effects, an important advantage in COX-2-targeted therapy, where CNS penetration is undesirable. However, celecoxib's higher Caco-2 permeability (0.839) compared to betanin and isobetanin (−1.094 for both) indicates a greater potential for systemic absorption, which, while beneficial for systemic inflammation, may be suboptimal for localized colonic delivery, as excessive systemic absorption could dilute the intended therapeutic effects.

Metabolic analysis reveals that celecoxib undergoes extensive biotransformation via cytochrome P450 (CYP) enzymes, including CYP3A4, CYP2D6, CYP2C9, and CYP1A2, leading to a higher risk of drug-drug interactions, increased metabolic burden, and potential side effects. In contrast, betanin and isobetanin demonstrate minimal interaction with CYP enzymes, signifying a simpler metabolic pathway, which may reduce the likelihood of metabolic interference and enhance safety in long-term use. Additionally, celecoxib exhibits the highest clearance rate (3.78 mL/min/kg), indicating rapid systemic elimination, whereas betanin (0.824 mL/min/kg) and isobetanin (0.898 mL/min/kg) demonstrate lower clearance rates, leading to prolonged retention in systemic circulation, which could be advantageous for sustained COX-2 inhibition and prolonged therapeutic effects in the colon. In addition, betanin and isobetanin exhibit a distinct advantage over celecoxib in terms of toxicity profile. The carcinogenicity, respiratory toxicity, and AMES mutagenicity scores of betanin and isobetanin are significantly lower than those of celecoxib, underscoring their potential as safer therapeutic alternatives, particularly under high-dose or long-term administration. This reduced toxicity is especially relevant for colorectal therapy, where prolonged anti-inflammatory intervention is often required and minimizing systemic adverse effects is essential.

Table 4 ADMET analysis of celecoxib, betanin, and isobetanin.

Parameters	Compounds		
	Celecoxib	**Betanin**	**Isobetanin**
Binding Affinity (kcal/mol)	−11.5	−8.6	−7.8
Molecular Weight	381.37	550.47	550.47
Absorpsition			
Log S	−4.720	−1.198	−1.281
Log P	3.072	−1.646	−1.666
Log D (7.4)	3.246	−0.423	−0.456
Log Kp (cm/s)	-6.21	−10.55	−10.55
HIA absorption	No	No	No
GI absorption (swiss)	High	Low	Low
Caco-2 Permeability (pkc)	0.839	−1.094	−1.094
MDCK permeability	−4.815	-4.976	−4.984
Distribution			
BBB permeability	No	No	No
Metabolism			
CYP3A4	Substrate	No	No
CYP2D6	Substrate	No	No
CYP2C9	Inhibitor	No	No
CYP1A2	Inhibitor	No	No
Excreation			
Clearance (Cl)	3.78	0.824	0.898
T½ (jam)	0.651	3.364	3.386
Toxicity			
Carcinogenicity	0.372	0.039	0.15
Respiratoty	0.787	0.22	0.124
AMES toxicity	0.306	0.114	0.314

Although betanin and isobetanin exhibit lower permeability and reduced gastrointestinal (GI) absorption compared to celecoxib, their encapsulation within an inulin-based drug delivery system presents a viable strategy to enhance bioavailability and ensure targeted colonic release. Inulin has been reported as a promising polysaccharide-based colon-targeted drug delivery system, making it particularly suitable for colorectal disease therapy [41-43]. Furthermore, the reduced CYP-mediated metabolism, lower systemic clearance, and superior safety profile of betanin and isobetanin further support their potential as alternative COX-2 inhibitors, offering a lower risk of adverse effects. These findings suggest that when formulated with inulin, betanin, and isobetanin could serve as effective and safer alternatives to celecoxib, particularly for targeted anti-inflammatory therapy in colorectal disease.

A comparative Lipinski's Rule of Five (Ro5) analysis of celecoxib, betanin, and isobetanin provides insights into their drug-likeness and pharmacokinetics (**Table 5**). Celecoxib, a clinically approved COX-2 inhibitor, aligns well with Lipinski's criteria, ensuring efficient oral absorption and distribution. With a

molecular weight of 381.37 g/mol, 4 rotatable bonds, and a TPSA of 86.36 Å², celecoxib exhibits favorable membrane permeability and bioavailability. Its 7 hydrogen bond acceptors and 1 donor support optimal protein binding, while moderate lipophilicity (log P = 3.072) enhances its systemic absorption.

Table 5 Lipinski's rule of 5 analysis for celecoxib, betanin, and isobetanin.

Lipinski Rules (SwissAdme)	Compounds		
	Celecoxib	**Betanin**	**Isobetanin**
Molecular Weight (gL/mol) (> 500)	381.37	550.47	550.47
Rotatable bonds	4	8	8
H-bond Acceptor (< 10)	7	14	14
H-bond Donor (< 5)	1	8	8
Molar Reefractivity	89.96	135.13	135.13
TPSA (Å²)	86.36	247.11	247.11
Violations	0	3	3

Conversely, betanin and isobetanin, with higher molecular weights (550.47 g/mol) and greater polarity (TPSA = 247.11 Å²), exhibit limited passive diffusion and reduced membrane permeability, which may hinder systemic absorption. However, their high hydrogen bonding capacity (14 acceptors, multiple donors) enhances aqueous solubility, supporting interaction with biomolecules. Their greater molecular flexibility (8 rotatable bonds) facilitates binding but may compromise stability. Inulin-based drug delivery addresses these limitations by enhancing colonic targeting and optimizing release and absorption at the COX-2 site of action. Although betanin and isobetanin slightly deviate from Lipinski's criteria, formulation with inulin enhances bioavailability and targeted delivery. Their safer toxicity profile, sustained colonic retention, and reduced metabolic interactions position them as viable alternatives to celecoxib for selective COX-2 inhibition.

Conclusions

In the 0.4 g betacyanin variation used for synthesizing betacyanin grafted inulin, the bound betacyanin content reached 582 mg BAE/g. FTIR analysis showed absorption bands at 1,540 - 1,418 cm^{-1}, corresponding to C=C stretching in the aromatic ring of betacyanin, and a peak at 1,670 cm^{-1} that indicated N-H bonds characteristic of the betalamic acid structure. UV Vis measurements confirmed a maximum absorption at 530 nm, consistent with the spectral properties of betacyanins. Antioxidant testing demonstrated that the 0.4 g variation retained a measurable antioxidant activity of 35.08 mg/L, suggesting that betacyanin remained bioactive after grafting onto inulin. Computational analysis supported these findings. Molecular docking and molecular dynamics simulations showed that betanin, the major constituent of betacyanin, had a binding affinity of −8.6 kcal/mol and a binding free energy of −20.3618 kcal/mol toward COX 2, indicating a stable interaction within the active site. ADMET profiling provided further insight into its pharmacokinetic properties. The compound showed good predicted oral absorption, favorable intestinal permeability, and acceptable distribution characteristics. Metabolic predictions suggested limited interaction with key cytochrome P450 enzymes, implying lower metabolic instability and reduced drug interaction risk. Toxicity modeling predicted low hepatotoxicity, low mutagenic potential, and an overall safe toxicity profile. Taken together, these results reinforce the therapeutic potential of betacyanins as natural compound-based candidates for colorectal cancer. When grafted onto inulin, the resulting matrix may improve colon targeted delivery and support COX 2 mediated anticancer activity, offering a promising strategy for colorectal cancer therapy.

Acknowledgements

The authors express their sincere gratitude to Universitas Negeri Padang for the support and research facilities provided. This work was financially supported

by PNBP UNP under research contract No. 987/UN35.13/LT/2022.

Declaration of generative AI in scientific writing

The authors acknowledge the use of generative AI tools (e.g., QuillBot and ChatGPT by OpenAI) to assist with language refinement and grammatical editing during manuscript preparation. These tools were not employed for content creation or data analysis. The authors retain full responsibility for the integrity, interpretation, and conclusions presented in this work.

CRediT author statement

Minda Azhar: Conceptualization; Methodology, Writing - Reviewing and Editing; Supervision; Project administration; Funding acquisition. **Selvi Apriliana Putri**: Data curation; Visualization; Investigation; Writing - Original draft preparation. **Iman Permana Maksum:** Validation. **Rendi Ananda**: Data curation; Investigation. **Muhammad Habibul Ikhsan**: Writing - Original draft preparation. **Anni Faridah**: Validation. **Hastria Effendi**: Validation. **Fatma Sri Wahyuni**: Validation.

References

[1] IG Yanti, M Azhar, A Faridah and B Oktavia. Simple determination of inulin polymerization degre average from dahlia tuber using spectrophotometer. *International Journal of Research and Review* 2019; **6**, 399-404.

[2] F Afinjuomo, S Abdella, SH Youssef. Inulin and its application in drug delivery. *Pharmaceuticals* 2021; **14**, 1-37.

[3] PV Dangre, KS Kotkar, AD Pimple and SS Meshram. Chemistry, isolation, and pharmaceutical applications of inulin. *Current Drug Therapy* 2025; **20(1)**, 8-17.

[4] BF Hinnebusch, S Meng, JT Wu, SY Archer and RA Hodin. The effects of short-chain fatty acids on human colon cancer cell phenotype are associated with histone hyperacetylation. *Journal of Nutrition* 2002; **132**, 1012-1017.

[5] Q Yang, J Ouyang, F Sun and J Yang. Short-chain fatty acids: A soldier fighting against inflammation and protecting from tumorigenesis in people with diabetes. *Frontiers in Immunology* 2020; **11**, 590685.

[6] G Liu, J Tang, J Zhou and M Dong. Short-chain fatty acids play a positive role in colorectal cancer. *Discover Oncology* 2024; **15(1)**, 425.

[7] N Gupta, AK Jangid, D Pooja and H Kulhari. Inulin: A novel and stretchy polysaccharide tool for biomedical and nutritional applications. *International Journal of Biological Macromolecules* 2019; **132**, 852-863.

[8] S Imran, RB Gillis, MS Kok, SE Harding and GG Adams. Application and use of inulin as a tool for therapeutic drug delivery. *Biotechnology and Genetic Engineering Reviews* 2012; **28(1)**, 33-46.

[9] J Sheng, H Sun, FB Yu, B Li, Y Zhang and YT Zhu. The role of cyclooxygenase-2 in colorectal cancer. *International Journal of Medical Sciences* 2020; **17(8)**, 1095-1101.

[10] RR Negi, SV Rana, V Gupta, R Gupta, VD Chadha, KK Prasad and DK Dhawan. Over-expression of Cyclooxygenase-2 in colorectal cancer patients. *Asian Pacific Journal of Cancer Prevention* 2019; **20(6)**, 1675-1681.

[11] Y Liu, H Sun, M Hu, Y Zhang, S Chen, S Tighe and Y Zhu. The role of cyclooxygenase-2 in colorectal carcinogenesis. *Clinical Colorectal Cancer* 2017; **16**, 165-172.

[12] J Liu, JF Lu, J Kan, XY Wen and CH Jin. Synthesis, characterization and *in vitro* anti-diabetic activity of catechin grafted inulin. *International Journal of Biological Macromolecules* 2014; **64**, 76-83.

[13] FH Pratama and M Azhar. Quercetin grafted inulin: Synthesis and characterization. *AIP Conference Proceedings* 2023; **2673**, 030001.

[14] HMC Azeredo. Betalains: Properties, sources, applications, and stability: A review. *International Journal of Food Science and Technology* 2009; **44**, 2365-2376.

[15] E Coy-Barrera. *Analysis of betalains (betacyanins and betaxanthins). In*: AS Silva, SF Nabavi and SM Nabavi. Recent advances in natural products analysis. Elsevier, Asterdam, Netherlands, 2020, p. 593-619.

[16] HY Leong, CW Ooi, CL Law, AL Julkifle, T Katsuda and PL Show. Integration process for betacyanins extraction from peel and flesh of

Hylocereus polyrhizus using liquid biphasic electric flotation system and antioxidant activity evaluation. *Separation and Purification Technology* 2019; **209**, 193-201.

[17] A Saber, N Abedimanesh, MH Somi, AY Khosroushahi and S Moradi. Anticancer properties of red beetroot hydro-alcoholic extract and its main constituent; betanin on colorectal cancer cell lines. *BMC Complementary Medicine and Therapies* 2023; **23(1)**, 246.

[18] MI Khan. Stabilization of betalains: A review. *Food Chemistry* 2016; **197**, 1280-1285.

[19] Q Chen, J Huang, J Gou, Q Ren and L Yuan. Inulin as carriers for renal targeting delivery of ferulic acid. *International Journal of Biological Macromolecules* 2020; **154**, 654-660.

[20] F Afinjuomo, S Abdella, SH Youssef, Y Song and S Garg. Inulin and its application in drug delivery. *Pharmaceuticals* 2021; **14(9)**, 855.

[21] AD Ergin, ZS Bayindir, M Gumustas, AT Ozcelikay and N Yuksel. A new strategy for enhancing S-Adenosyl-L-Methionine (SAMe) oral bioavailability: Preparation of SAMe loaded inulin nanoparticles for colon targeting with *in vivo* validation. *International Journal of Biological Macromolecules* 2025; **289**, 138818.

[22] W Akram, V Pandey, R Sharma, R Joshi, N Mishra, N Garud and T Haider. Inulin: Unveiling its potential as a multifaceted biopolymer in prebiotics, drug delivery, and therapeutics. *International Journal of Biological Macromolecules* 2024; **259**, 129131.

[23] B Hufnagel, V Muellner, K Hlatky, C Tallian, R Vielnascher, GM Guebitz, M Wirth and F Gabor. Chemically modified inulin for intestinal drug delivery - a new dual bioactivity concept for inflammatory bowel disease treatment. *Carbohydrate Polymers* 2021; **252**, 117091.

[24] F Fathordoobady, H Mirhosseini, J Selamat, M Yazid and A Manap. Effect of solvent type and ratio on betacyanins and antioxidant activity of extracts from Hylocereus polyrhizus flesh and peel by supercritical fluid extraction and solvent extraction. *Food Chemistry* 2016; **202**, 70-80.

[25] R Asra, RD Yetti, S Audina and N Nessa. Studi fisikokimia betasianin dalam kulit buah naga dan aplikasinya sebagai pewarna merah alami sediaan farmasi (*in Indonesian*). *Jurnal Farmasi Galenika* 2019; **5(2)**, 140-146.

[26] J Liu, J Lu, J Kan, X Wen and C Jin. International Journal of Biological Macromolecules Synthesis, characterization and *in vitro* anti-diabetic activity of catechin grafted inulin. *International Journal of Biological Macromolecules* 2014; **64**, 76-83.

[27] IB Slimen, T Najar and M Abderrabba. Chemical and antioxidant properties of betalains. *Journal of Agricultural and Food Chemistry* 2017; **65(4)**, 675-689.

[28] DB Rodriguez-amaya, S Paulo and F Sul. Update on natural food pigments - A mini-review on carotenoids, anthocyanins, and betalains. *Food Research International* 2018; **124**, 200-205.

[29] MI Khan and P Giridhar. Plant betalains: Chemistry and biochemistry. *Phytochemistry* 2015; **117**, 267-295.

[30] S Phongpaichit, J Nikom, N Rungjindamai, J Sakayaroj, N Hutadilok-Towatana, V Rukachaisirikul, & K Kirtikara. Biological activities of extracts from endophytic fungi isolated from Garcinia plants. *FEMS Immunology & Medical Microbiology* 2007; **51**(3), 517-525.

[31] H Shang, H Zhou, J Yang, R Li, H Song and H Wu. *In vitro* and *in vivo* antioxidant activities of inulin. *PloS One* 2018; **13(2)**, 1-12.

[32] S Putri, R Maharani, I Maksum and T Siahaan. Peptide design for enhanced anti-melanogenesis: Optimizing molecular weight, polarity, and cyclization. *Drug Design, Development and Therapy* 2025; **19**, 645-670.

[33] N Gupta, AK Jangid, D Pooja and H Kulhari. Inulin: A novel and stretchy polysaccharide tool for biomedical and nutritional applications. *International Journal of Biological Macromolecules* 2019; **132**, 852-863.

[34] S Joseph, M Jadav, R Solanki, S Patel, D Pooja and H Kulhari. Synthesis, characterization, and application of honey stabilized inulin nanoparticles as colon targeting drug delivery carrier. *International Journal of Biological Macromolecules* 2024; **263**, 130274.

[35] RM Garavito, MG Malkowski and DL Dewitt. The structures of prostaglandin endoperoxide H synthases-1 and-2. *Prostaglandins & Other Lipid Mediators* 2002; **68**, 129-152.

[36] AJ Vecchio and MG Malkowski. The structure of NS-398 bound to cyclooxygenase-2. Journal of Structural Biology. 2011; **176(2)**, 254-258.

[37] BJ Orlando and MG Malkowski. Substrate-selective inhibition of cyclooxygeanse-2 by fenamic acid derivatives is dependent on peroxide tone. *Journal of Biological Chemistry* 2016; **291**, 15069-15081.

[38] D Wang and RN Dubois. The role of COX-2 in intestinal inflammation and colorectal cancer. *Oncogen* 2010; **29**, 781-788.

[39] L Tesoriere, M Allegra, D Butera and MA Livrea. Absorption, excretion, and distribution of dietary antioxidant betalains in LDLs: potential health effects of betalains in humans. *The American Journal of Clinical Nutrition* 2004; **80(4)**, 941-945.

[40] A Pangal and K Ahmed. Synthesis and biological evaluation of coumarin-quinone hybrids as multifunctional bioactive agents. *ADMET and DMPK* 2023; **11**, 81-96.

[41] AK Philip and B Philip. Colon targeted drug delivery systems: A review on primary and novel approaches. *Oman Medical Journal* 2010; **25**, 70-78.

[42] AH Teruel, I Gonzalez-Alvarez, M Bermejo, V Merino, MD Marcos, F Sancenon, M Gonzalez-Alvarez and R Martinez-Mañez. New insights of oral colonic drug delivery systems for inflammatory bowel disease therapy. *International Journal of Molecular Sciences* 2020; **21(18)**, 6502.

[43] H Shao, M Liu, H Jiang and Y Zhang. Polysaccharide-based drug delivery targeted approach for colon cancer treatment: A comprehensive review. *International Journal of Biological Macromolecules* 2025; **302**, 139177.

Supplementary materials

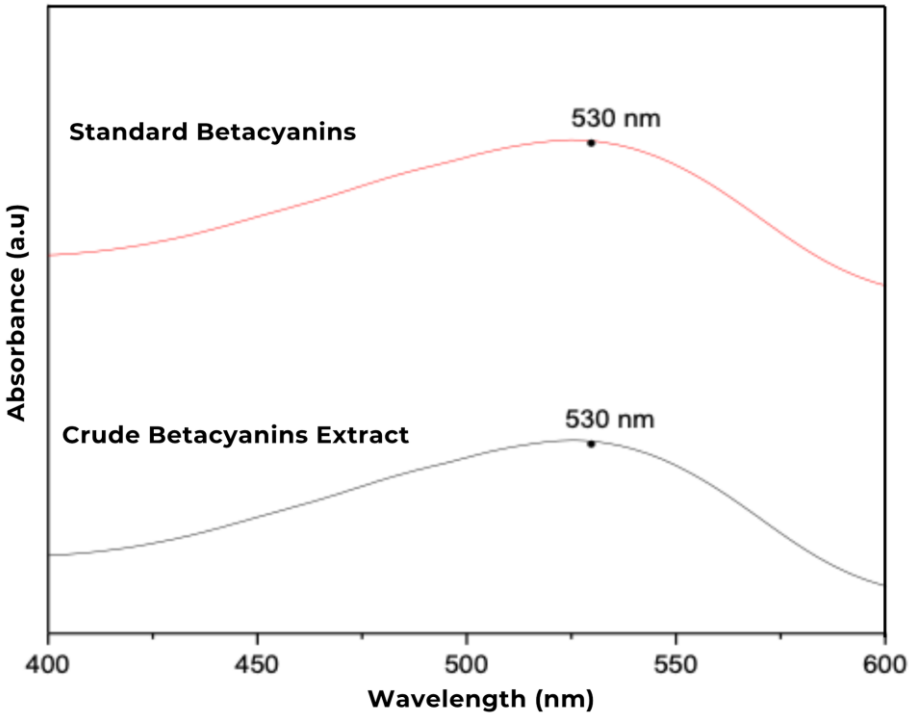

Figure S1 UV-Vis spectra of betacyanin (betanin) and betacyanins extract.

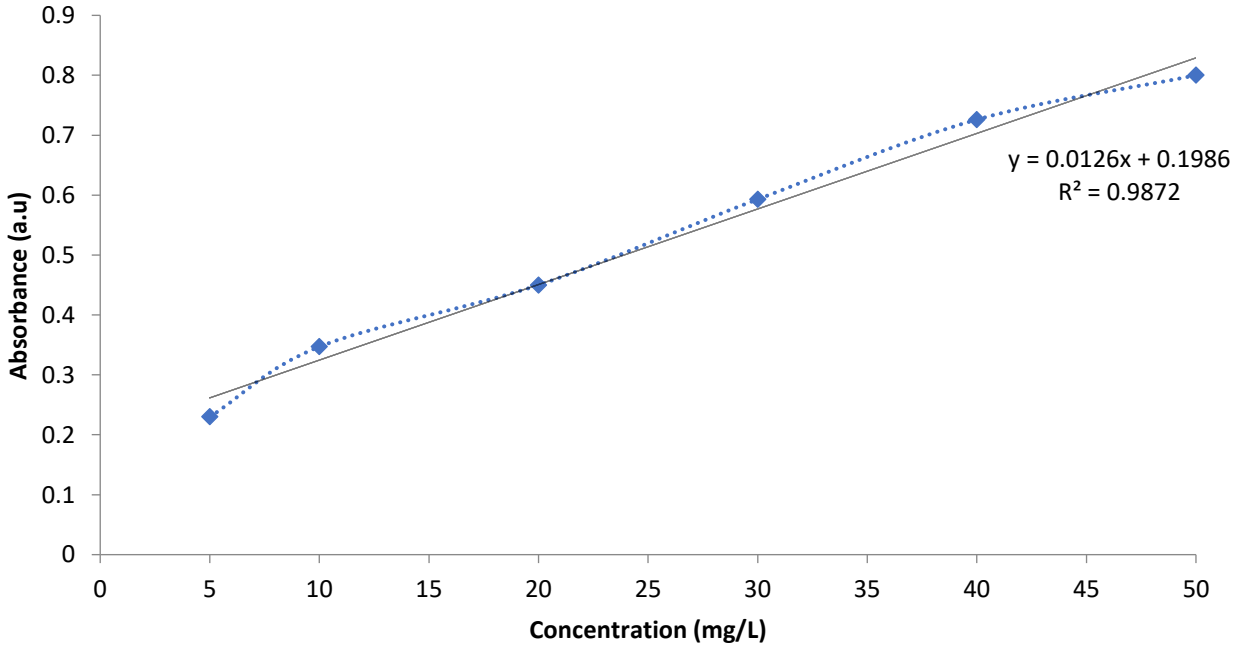

Figure S2 Standard curve of betacyanin (Betanin).

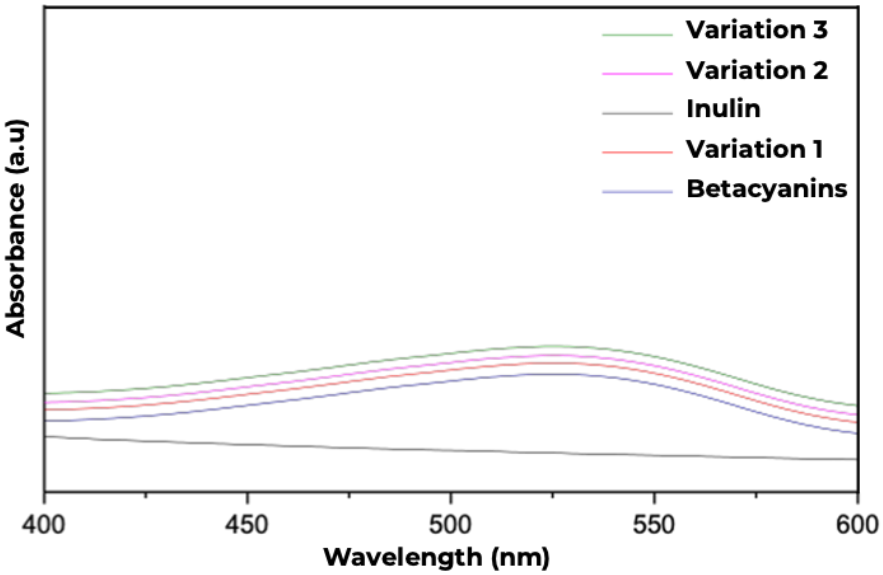

Figure S3 UV-Vis Spectra of Inulin, Betacyanins, and Betacyanin-Grafted Inulin.

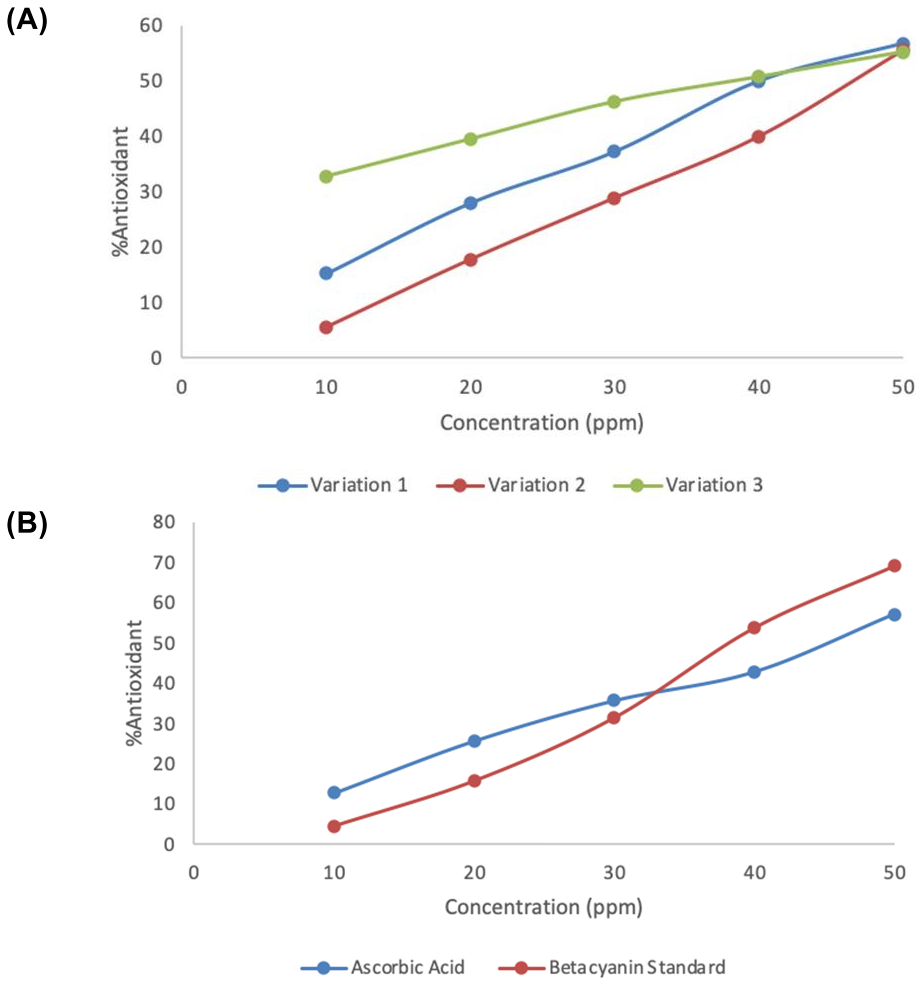

Figure S4 Correlation curve between concentration and antioxidant percentage. This figure illustrates the relationship between concentration and antioxidant activity (%) for different samples: (A) Synthesis Variation 1, Synthesis Variation 2 and Synthesis Variation 3, (B) Ascorbic Acid (positive control), and Betacyanin Standard, highlighting the differences in radical scavenging efficiency across the tested variations.